Available online at www.sciencedirect.com

ScienceDirect

Procedia Engineering 105 (2015) 877 – 884

Procedia Engineering

www.elsevier.com/locate/procedia

6th BSME International Conference on Thermal Engineering (ICTE 2014)

# Characteristics of pulsatile blood flow through 3-D geometry of arterial stenosis

Khairuzzaman Mamun[a], Most. Nasrin Akhter[a] *, Md. Shirazul Hoque Mollah[a]

Md. Abu Naim Sheikh[a], Mohammad Ali[b]

[a]*Department of Mathematics, Dhaka University of Engineering and Technology, Gazipur-1700, Bangladesh.*
[b]*Department of Mechanical Engineering, Bangladesh University of Engineering and Technology, Dhaka-1000, Bangladesh.*

**Abstract**

A numerical simulation is carried out to demonstrate the significant changes of flow behaviour for two different severities of arterial stenosis. Two stenosis levels of 65% and 85% are considered by area. The blood is considered as flowing fluid and assumed to be incompressible, homogeneous and Newtonian, while artery is assumed to be a rigid wall. The transient analysis is performed using ANSYS-14.5. The flow pattern, wall shear stress (WSS), pressure contours, and Centre-line velocity distribution are observed at early-systole, peak-systole and diastole for better understanding of arterial disease. Wall Share Stress distribution shows that as severity increases, sharing of flow also increases for all cases. Thus maximum stress is exerted in throat region at peak systole. The pressure distribution demonstrates that at all cases 85% stenotic artery creates more force than 65% stenotic artery at their pre-stenotic region. Interestingly, a recirculation region is visible at the post stenotic region in 85% stenotic artery for all cases and recirculation region increases with the decrease of the inlet flow velocity. Analysis indicates that the significant flow changes happen in the post stenotic region.


Peer-review under responsibility of organizing committee of the 6th BSME International Conference on Thermal Engineering (ICTE 2014)

*Keywords: Stenosis; pulsatile flow; recirculation region; wall shear stress.*

* Corresponding author. Tel.: +88-01749-288044;
*E-mail address:* nasrin6092002@yahoo.com


Peer-review under responsibility of organizing committee of the 6th BSME International Conference on Thermal Engineering (ICTE 2014)
doi:10.1016/j.proeng.2015.05.090

## 1. Introduction

Cardiovascular diseases are the types of diseases that involve heart or blood vessels (arteries and vain). On the other hand, stenosis is a constriction in the blood vessels, and causes stroke and even fatal death of human life. We have limited understanding on this issue. Therefore, studies of stenosis can be helpful better understanding of the biomechanics of vascular diseases. In general the blood flow should not face any obstacles on the way and the flow should be regular and smooth. But sometimes due to presence of cholesterol, calcium and other substance in blood, a fatty substance called plaque develops near the inner wall of the artery. As the time passes this plaque grows resulting in hardening the arterial wall and narrowing the blood vessels. This can cause severe diseases such as the development of atherosclerosis. As a result the arterial wall loses its elastic property which limits the area of blood flow. Therefore, the flow turns to show abnormal behavior in the reduced cross sectional area of the artery as shown by Khader and Shenoy [1]. The studies suggested that pulsatile blood flow through artery vessel implicated in several types of hemodynamic forces that could impact in vessel wall structure. These forces caused the development of vascular pathologies and atherosclerosis. The high shear stress was the harm of the vessel wall and caused atherosclerosis. Therefore, the vessel with steady blood flow and high shear stress was good for health and comparatively free of the above diseases as investigated by Li et al. [2].

At present, there is no standard procedure to measure the physical severity of the stenosis. Doctors often judge the severity of the above diseases based on a patient's physical symptoms as well as growth rate, constriction size and pressure drop as stated by Chua, and Shread [3]. However the results of numerical simulation could be an important technique with others like MR, CT, and Ultrasound etc. in analyzing the severity of stenosis. Further the comparison of stenosed flow behaviour with the normal one can provide the better understanding of underlying mechanism behind the development of atherosclerosis. The flow behaviour in the stenosed artery is quite different in comparison to the normal one. On the other hand, stress and resistance to flow are much higher in stenosed artery than one in the normal artery. Chua & Shread et al [3] proved that the flow through the constricted tube was characterized by high velocity jet generated in constricted region and flow separation downsream to the stenosis. Khader & Shenoy et al. [1] found that velocity and stenotic jet length increases with the increase in the severity of stenosis. Young et al. [4] studied the wall shear stress and pressure gradient in the stenosis and evaluated the cause of plaque rupture. They founded pulsatile blood flow through the stenosis with elastic wall to observe the lumen movement. According to their study the peak WSS occurred just before minimum lumen position. Pinto et al. [5] conducted numerical simulation assuming a physiological pulsatile flow through different models of stenosis. In case of anatomically realistic stenosed carotid bifurcation subjected to pulsatile inlet condition, the simulation results demonstrated the rapid fluctuation of velocity and pressure in post-stenotic region as showed by S. Lee et al. [7]. Ahmed and Giddens [6] studied both steady and pulsatile flow through 25%, 50% and 75% constriction of a rigid tube where Reynolds number ranges from 500 to 2000 using Laser Doppler Anemometry (LDA). Sinonusoidal pulsatile turbulent flow through a rigid wall stenotic vessel was numerically modelled using Reynolds Averaged Navier –Stokes equation approach by Varghese & Frankel [8]. The authors showed that low Reynolds number $k-\omega$ turbulence model had better agreement with the results of Ahmed and Giddens [6].

The above mentioned previous experimental and computational results made the analysis on the flow aspects in proximal and distal end of stenosis including a detailed observation. Apart from this, an attempt is made in this study to demonstrate the significant changes of flow behaviour for 65 and 85 percentages severities of stenosis. For simulation RANS based standard $k-\omega$ turbulent model with low Reynolds correction is used. Detailed investigation of flow parameters like velocity, Wall Share Stress and pressure contours are discussed. The working domain and the boundary conditions of the geometry are defined in pre-processor software ANSYS Workbench. The Finite volume analysis is performed using ANSYS Fluent-14.5.

**Nomenclature**

| | | | |
|---|---|---|---|
| D | diameter of the healthy artery | x | axial location of the flow field |
| r | radial location of the flow field | T | time period of the inlet flow cycle |
| R | radius of the healthy artery | u | instantaneous velocity |
| U | average velocity | WSS | wall shear stress |

## 2. Mathematical model

The Reynolds Averaged Navier-Stokes (RANS) equations are used to solve the problem numerically. The working fluid is blood which is assumed to be incompressible, Newtonian with constant viscosity and density. The heat transfer in the blood flow process is not considered. Therefore energy equation is not solved. The system of equations can be given by

$$\frac{\partial u_i}{\partial x_i} = 0 \tag{1}$$

$$\rho \frac{\partial u_i}{\partial t} + \rho \frac{\partial}{\partial x_j}(u_j u_i) = -\frac{\partial p}{\partial x_i} + \frac{\partial}{\partial x_j}(2\mu s_{ij}) \tag{2}$$

where, the strain-rate tensor $S_{ij}$ is given by,

$$s_{ij} = \frac{1}{2}\left( \frac{\partial u_i}{\partial x_j} + \frac{\partial u_j}{\partial x_i} \right) \tag{3}$$

Due to constriction, the flow velocity at post stenotic region increases and accordingly the pressure decreases. For this region, turbulent flow is expected at post stenotic region especially for 85% stenotic artery. The two-equations low Re $k-\omega$ turbulence model of was chosen. Unlike any other model the $k-\omega$ model is more acceptable for flow analysis by Varghese & Frankel [8].

The turbulence kinetic energy $k$ and specific dissipation rate $\omega$ of standard $k-\omega$ model are determined by following two equations:

The $k$ equation: $$\frac{\partial}{\partial t}(\rho k) + \frac{\partial}{\partial x_i}(\rho k u_i) = \frac{\partial}{\partial x_j}\left( \Gamma_k \frac{\partial k}{\partial x_i} \right) + G_k - Y_k + S_k \tag{4}$$

The $\omega$ equation: $$\frac{\partial}{\partial t}(\rho \omega) + \frac{\partial}{\partial x_i}(\rho \omega u_i) = \frac{\partial}{\partial x_j}\left( \Gamma_\omega \frac{\partial k}{\partial x_i} \right) + G_\omega - Y_\omega + S_\omega \tag{5}$$

In these equations, $G_k$ represents the generation of turbulence kinetic energy due to mean velocity gradients. $G_\omega$ represents the generation of $\omega$. $\Gamma_k$ and $\Gamma_\omega$ represent the effective diffusivity of $k$ and $\omega$, respectively. $Y_k$ and $Y_\omega$ represent the dissipation of $k$ and $\omega$ due to turbulence. $S_k$ and $S_\omega$ are user-defined source terms.

A low Reynolds number correction factor controls the influence on the overall structure of the flow field, depending upon local conditions, and it is given as

$$\nu_t = \alpha^* \frac{k}{\omega} \qquad \alpha^* = \frac{\alpha_0^* + \mathrm{Re}_t/R_k}{1 + \mathrm{Re}_t/R_k} \qquad \alpha = \frac{5}{9}\frac{\alpha_0 + \mathrm{Re}_t/R_\omega}{1 + \mathrm{Re}_t/R_\omega}(\alpha^*)^{-1} \qquad \beta^* = \frac{9}{100}\frac{5/18 + (\mathrm{Re}_t/R_\beta)^4}{1 + (\mathrm{Re}_t/R_\beta)^4} \tag{6}$$

Closure Coefficient for the $k-\omega$ Model are

$$\beta = \frac{3}{40}, \quad \sigma^* = \sigma = 0.5, \quad \alpha_0^* = \frac{\beta}{3}, \quad \alpha_0 = 0.1,\ R_k = 6, \quad R_\omega = 2.7, \quad R_\beta = 8 \tag{7}$$

### *2.1 Model description*

Three dimensional stenotic arteries are used as geometry for this study shown in Fig. 1 (a). For this study, two geometries of 65% and 85% stenotic artery (by area) are taken. The geometry of generated model in this study has a diameter (D) of 6 mm and a length (L) of 84 mm, where the length of pre-stenotic, throat and post stenotic region are 4D, 2D and 8D respectively. The wall is considered to be rigid. The flow field mesh consists of 39423 nodes and 82580 elements for 65% stenotic artery and of 40873 nodes and 85777 elements for 85% stenotic artery. Figure 1(b) shows the mesh in cross sectional inflow plane of a stenotic artery.

Grid dependency study is the first preference of any numerical simulation. For this purpose an extensive test is carried out with different sizes of mesh such as mesh0 (75511 element), mesh1 (82580 element) and mesh2 (90227 element) respectively. Fig 1(c) shows the pressure distributions for 65% stenosis artery with mentioned mesh sizes. In all cases, the pressure distributions are same. It implies that the solution is grid independence.

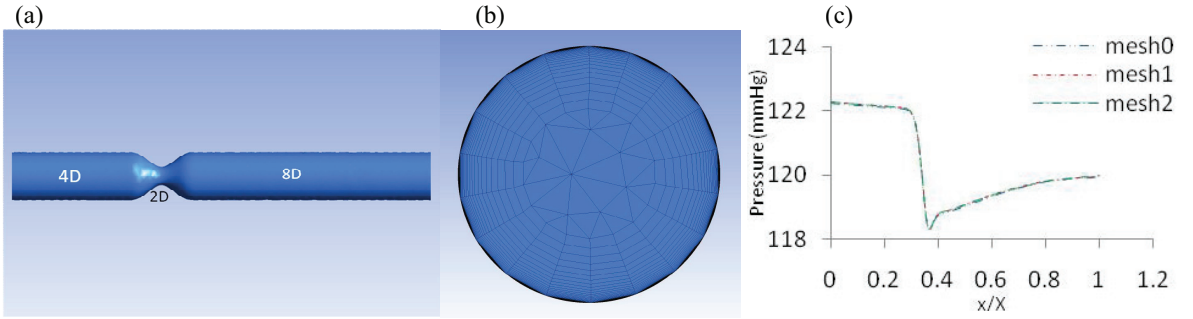


Fig 1. (a) Model of stenotic artery; (b) mesh in cross sectional inflow plane of stenotic artery (c) Grid sensitivity study

### *2.2 Boundary condition*

In this study, the unsteady parabolic velocity profile at inlet and the unsteady flat pressure profile at outlet have been imposed for boundary condition, using the equation (8) and (9) respectively.

$$u_x = (u_0 + u_m \sin(\omega t))\left(1 - \frac{y^2 + z^2}{radius^2}\right) \tag{8}$$

$$p = p_0 + p_m \sin(\omega t) \tag{9}$$

Here, $u_0$ and $u_m$ values are taken according to the flow field Reynolds number which varies from 200 to 1200. Similarly, pressure varies from 80 mmHg to 120 mmHg. Fig. 2(a) and 2(b) show the unsteady and parabolic inlet velocity profile. In figure 2(a); a, b, and c represent the positions of early systole, peak systole, and diastole respectively. Blood is taken as fluid and considered as incompressible and Newtonian. The density and viscosity of the blood are 1050kg/m$^3$, and 0.004N-sec/m$^2$ respectively.

### *2.3 Numerical Scheme*

The numerical simulations are performed by well known software ANSYS Fluent 14.5. A pressure based algorithm is chosen as the solver type. This solver is generally selected for an incompressible fluid. As there is no heat transfer in the blood flow process, energy equation is not solved. Since turbulent is expected in 85% stenotic artery at post stenotic region, a $k-\omega$ turbulent model is used throughout the work. In solution methods, the SIMPLE algorithm is selected for pressure-velocity coupling. First Order Upwind scheme is employed as a numerical scheme for discretization of the momentum equation. The time step is set to 0.0041 sec with 200 number of total time steps. Maximum 100 iterations are performed per each time step.

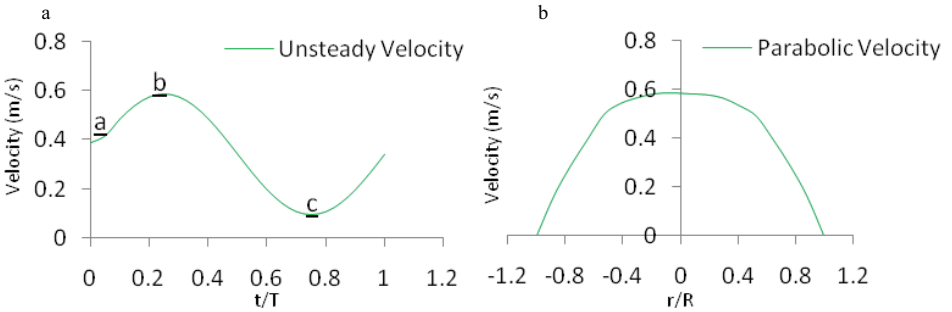


Fig 2. (a) Time dependent and (b) parabolic inlet velocity profile.

*2.4 Validation*

Before starting of present investigation, the numerical code validation is needed. For validation, the study of Varghese & Frankel [8] is considered. For this case, 75% (by area) stenotic artery is taken as geometry, and a parabolic velocity profile is assumed as inlet boundary condition. The mean inlet velocity corresponds to Reynolds number 500 and the flow is assumed to be steady. The comparison of velocity profile at 2.5D downstream from the stenosis throat is shown in Fig.3 and a good agreement can be found with Varghese & Frankel [8]. In spite of little discrepancies, the qualitative agreement is found.

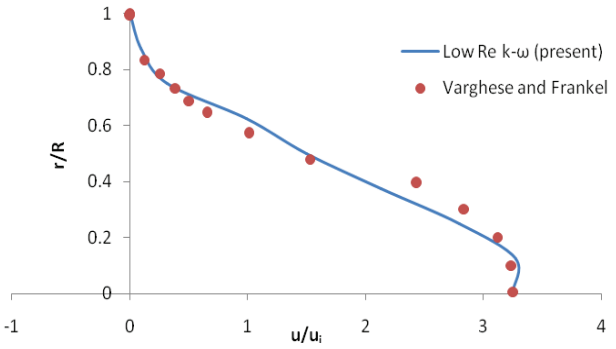


Fig. 3: Comparison of computed steady velocity profile.

## 3. Results and discussion

The computational results are conducted to study the influence of stenosis on the flow behaviour. The flow parameters like velocity, pressure, WSS are observed from transverse and longitudinal contours at specific instants of pulse cycle for comparing the flow variation. The discussion is categorized with the observations of flow variation starting from early systole, peak systole and diastole, respectively.

*3.1 Effect of stenosis on the wall shear stress*

Generally, WSS is an important factor to determine the effect of severity of arterial stenosis. It depends on the viscosity of the fluid and velocity gradient and, is defined as $\tau = \mu \frac{du}{dr}$, where $\mu$ is the viscosity and $\frac{du}{dr}$ is the velocity gradient.

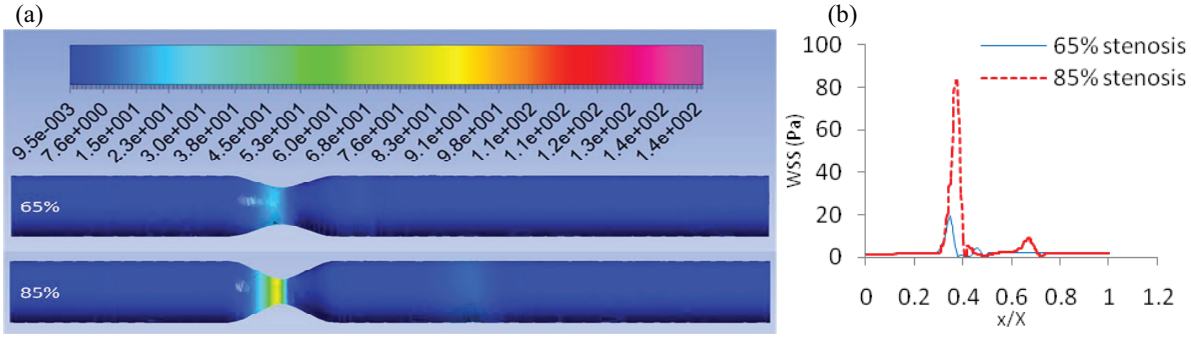


Fig. 4: (a) WSS in 65% and 85% stenotic arteries contour at early systole and (b) comparison of WSS distribution at early-systole

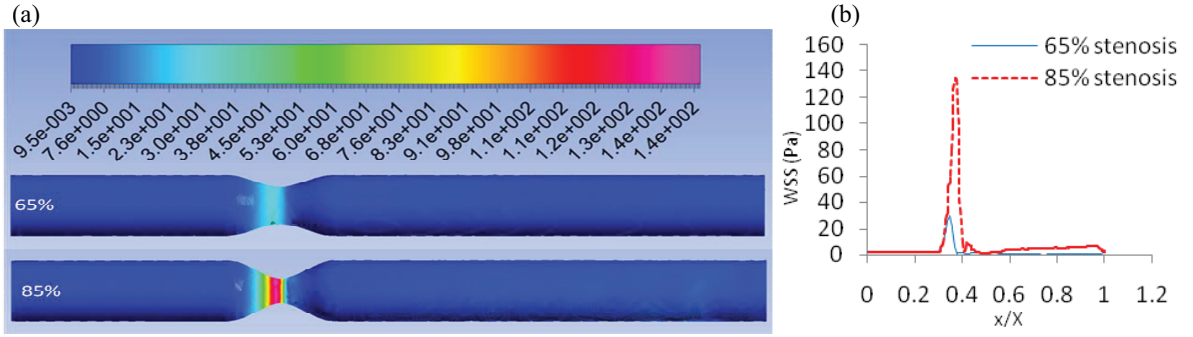


Fig. 5: (a) WSS in 65% and 85% stenotic arteries contour at peak systole and (b) comparison of WSS distribution at peak-systole

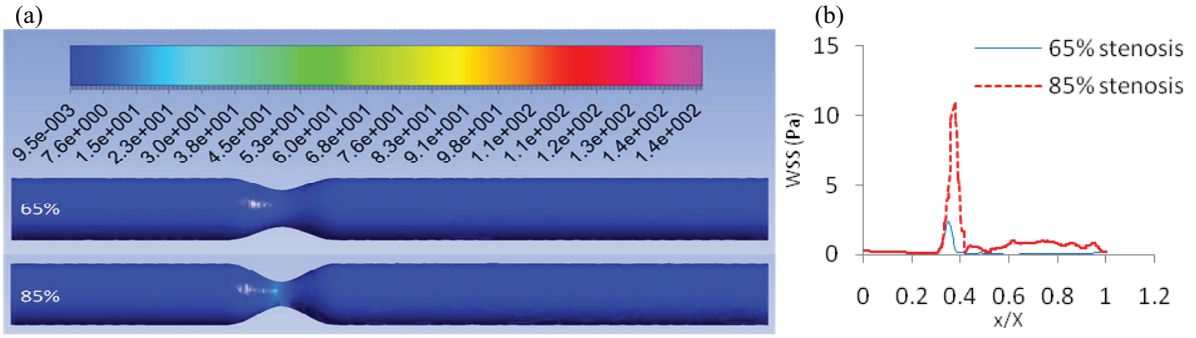


Fig. 6: (a) WSS in 65% and 85% stenotic arteries contour at diastole and (b) comparison of WSS distribution at diastole.

Figures, 4(a), 5(a), 6(a) show the contours of WSS in 65% and 85% stenotic arteries and Figs.4(b), 5(b), 6(b) show the comparisons of WSS in both stenotic artery at early-systole, peak systole and diastole respectively. In both severities, WSS is uniformly distributed at pre and post stenotic regions. The results reveal that the flow pattern changes abruptly in all cases at the region of stenosis throat onwards in the downstream whereas no significant change is observed in the upstream and it is significantly observed that the changes of WSS is due to increase of severities. Surprisingly a sharp raise of WSS and immediately decline are observed in the stenotic throat. From the comparisons, our finding is that maximum WSS is observed at peak systole and 85% severity. No mentionable change is observed at early systole and diastole in both severities.

### *3.2 Effect on pressure and velocity flow field*

Pressure distributions in both stenotic arteries at early-systole, peak-systole, and diastole are shown in Figs. 7, 8, and 9 respectively, and Centre-line velocity distribution at early-systole, peak-systole and diastole is shown in Fig. 10.

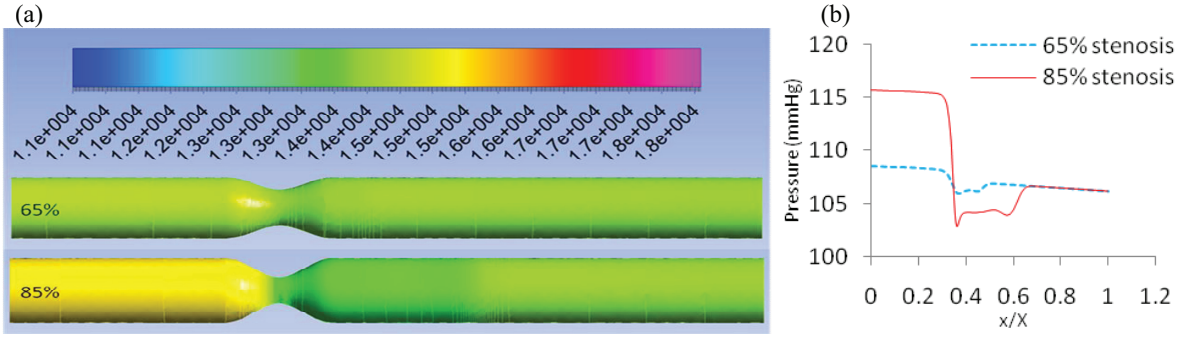


Fig. 7: (a) Pressure in 65% and 85% stenotic arteries contour at early systole and, (b) comparison of pressure distribution at early systole.

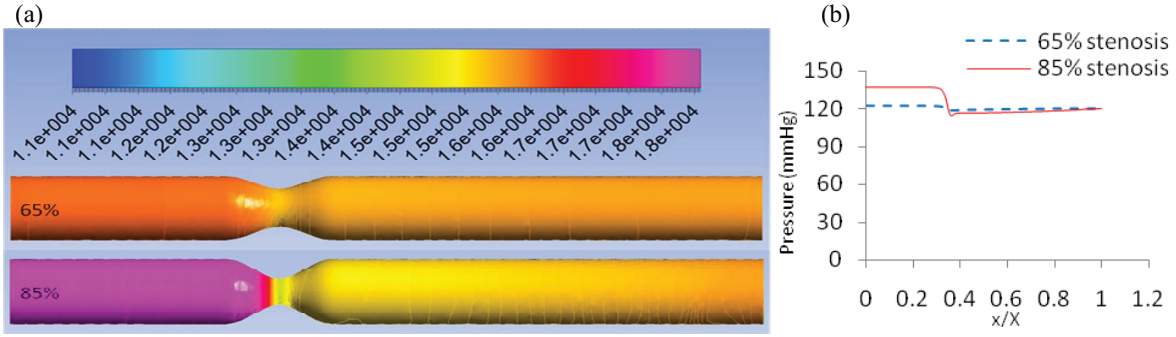


Fig. 8: (a) Pressure in 65% and 85% stenotic arteries contour at peak systole and, (b) comparison of pressure distribution at peak systole.

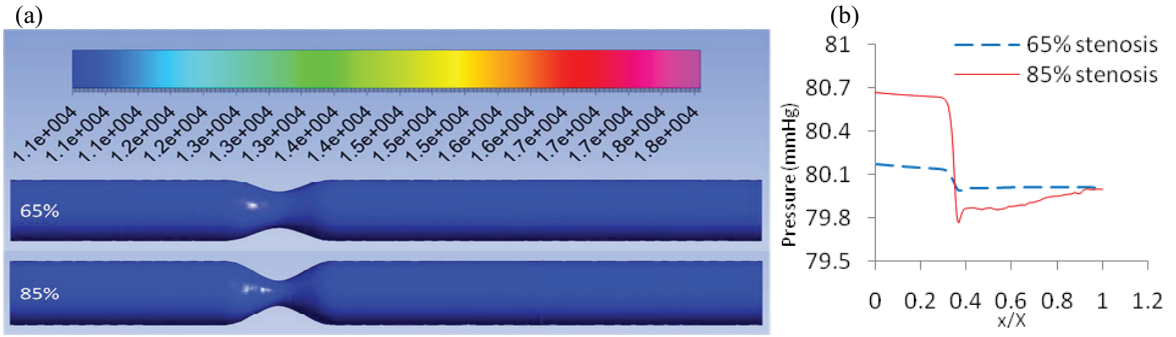


Fig. 9: (a) Pressure in 65% and 85% stenotic arteries contour at diastole and, (b) comparison of pressure distribution at diastole.

Figure 7(a) shows the contour of pressure in 65% and 85% stenotic arteries at early-systole. In 65% stenotic artery the pressure is uniform and is varying with a small variation throughout the geometry. High pressure at pre-stenotic region and sudden decline of the pressure at the throat are characterized in 85% stenotic artery. Again, Fig. 7(b) shows that the pressure at inlet and throat for 65% stenotic artery are 108.55 mmHg and 106.00 mmHg and for 85% stenotic artery are 115.75 mmHg and 102.84 mmHg respectively. Fig. 8(a) shows the distribution of pressure in 65% and 85% stenotic arteries at peak-systole. Furthermore, it describes almost same interpretation as figs. 7(a). But Fig. 8(b) implies that the pressure at inlet and throat for 65% stenotic artery are 122.29 mmHg and 118.46 mmHg and for 85% stenotic artery are 137.42 mmHg and 114.47 mmHg respectively. During calculation, at first standard condition is taken in pressure boundary condition such as diastolic & systolic blood pressure as 80 mmHg & 120 mmHg respectively. But From Fig, 8, it is noticed that the systolic pressure at pre stenotic region for both severities raise from 120 mmHg to 122.29 mmHg & 137.42 mmHg respectively. The results clearly noticed that 85% arterial stenosis can cause fatal death by blasting the pre stenotic arterial region of the patient of high blood pressure. Fig. 9(a) shows the contours of pressure in 65% and 85% stenotic arteries at diastole. From Fig. 9(a), we observe that, pressure is uniform and changing with a small variation at the throat. From 9(b), it is observed that, the pressure at inlet and throat for 65% stenotic artery are 80.17 mmHg and 80.00 mmHg and for 85% stenotic artery are 80.66 mmHg and 79.77 mmHg respectively. It is well known that pressure difference may provide some kind of extra force that may drive blood through the stenosis with high velocity. Since The pressure difference in 85% stenotic artery is higher than that of 65% stenotic artery for all case. So at every case 85% stenotic artery creates more force than 65% stenotic artery at their pre-stenotic region.

In Fig. 10, inlet velocity in both geometries begins with same magnitude for all case. Velocities at the throat and post stenotic region for all cases of 85% stenotic artery are relatively higher than that of 65% stenotic According artery. Recirculation region is observed in 85% stenotic artery at post stenotic region for all cases. In the other hand, velocity is laminar in 65% stenotic artery at post stenotic region for all cases. The highest velocity is observed in 85% stenotic artery at peak systole and the lowest velocity is observed in 65% stenotic artery at diastole.

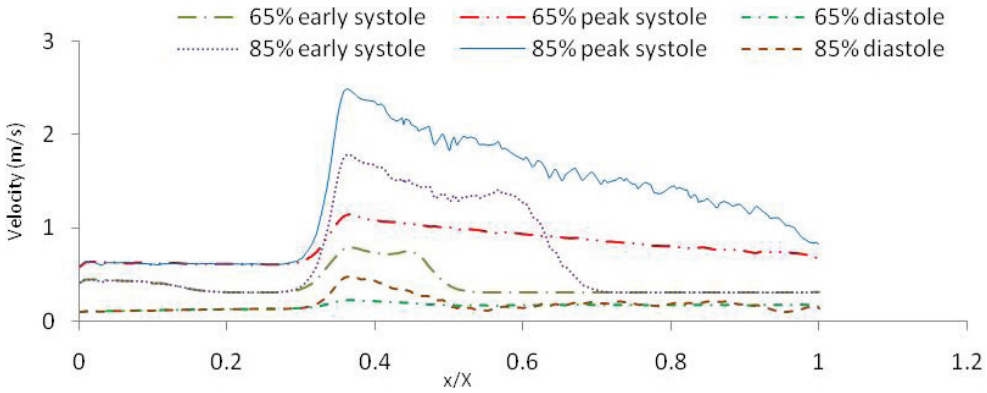


Fig. 10: Centre-line velocity distribution at early-systole, peak-systole and diastole.

## 4. Conclusion

A numerical study on pulsatile blood flow through 3-D stenotic artery is performed. Pressure and velocity flow field, and wall shear stress occurred in the flow field are analysed. The wall share stress distribution shows that as the stenotic severity increases, share stress of flow increases for all cases. The maximum stress occurs at throat region at peak systole. The pressure distribution demonstrates that at every case 85% stenotic artery creates more pressure than 65% stenotic artery at pre-stenotic region and 85% arterial stenosis can cause fatal death by blasting the pre-stenotic arterial region of the patient of high blood pressure. The results demonstrate that the velocity increases in throat region with the increase in stenotic severity for all cases. A recirculation region is visible at the post-stenotic region in 85% stenotic artery for all cases and recirculation region increases with the decrease of the inlet flow velocity.

**References**:

[1] S. Khader, and B. Shenoy; Effect of increased severity in patient specific stenosis, World Journal of Modelling and Simulation, Vol. 7 (2011) No. 2, pp. 113-122.

[2] M.X. Li, J.J. Beech-Brandt, L.R. John, P.R. Hoskins, and W.J. Easson, Numerical analysis of pulsatile blood flow and vessel wall mechanics in different degrees of stenosis, J. Biomech, 40 (2007) 3715-3724

[3] C. Chua, and G. Shread, Changes in flow and wall stresses through arterial constriction offset from the centre of the vessel, The Anziam Journal, 2009, 50: C744–C759.

[4] V. Young, A. Patterson M. Graves, Z-Y LI, V. Tavani, T. Tang, and J. H. Gillard, The mechanical triggers of rupture: shear vs pressure gradient, The British J. of Radiology, 82 (2009) S39-S45

[5] J. Pinto, K.L. Bessa, D.F. Legendre, and R.H. Mouth, Physiologycal pulsatile waveform through axisymmetric stenosed arteries: Numerical Simulation, ABCM Symposium in Bioengineering, 1 (2006).

[6] S.A. Ahmed, and D.P. Giddens, Pulsatile Poststenotic Flow Studies with Laser Doppler Anemometry, J. Biomech., 17 (1984) 695-705.

[7] S. Lee, and S. Lee, Direct numerical simulation of transitional flow in a stenose carotid bifurcation, Journal of Biomechanics, 2008, 41: 2551–2561.

[8] S.S. Varghese and S.H. Frankel, Numerical Modeling of Pulsatile Turbulent Flow in Stenotic Vessels, J. Biomech, Vol. 125, pp. 445-460, 2003.

[9] Zuned Mansuri, Pulsatile Blood Flow Simulations in Computed Tomography (CT) Scan-Based and Idealized Geometries of Human Aorta, Lappeenranta University of Technology, Department of Mathematics and Physics(2010).

[10] S.R. Shahed, Md. Ali, S. Saha, and M.N. Akhter, Numerical study on unsteady flow field of arterial stenosis, Presented in the Int. conference on Mechanical Engg. (ICME 2013), 20-21 June, 2014, Dhaka-1000, Bangladesh, and will be published in Procedia Engineering (2014), Elsevier, SciVerse ScienceDirect.